



**HAL**  
open science

## Polypeptides derived from $\alpha$ -Synuclein binding partners to prevent $\alpha$ -Synuclein fibrils interaction with and take-up by cells

Elodie Monsellier, Maya Bendifallah, Virginie Redeker, Ronald Melki

### ► To cite this version:

Elodie Monsellier, Maya Bendifallah, Virginie Redeker, Ronald Melki. Polypeptides derived from  $\alpha$ -Synuclein binding partners to prevent  $\alpha$ -Synuclein fibrils interaction with and take-up by cells. PLoS ONE, 2020, 10.1371/journal.pone.0237328 . cea-02915659

**HAL Id: cea-02915659**

**<https://cea.hal.science/cea-02915659v1>**

Submitted on 15 Aug 2020

**HAL** is a multi-disciplinary open access archive for the deposit and dissemination of scientific research documents, whether they are published or not. The documents may come from teaching and research institutions in France or abroad, or from public or private research centers.

L'archive ouverte pluridisciplinaire **HAL**, est destinée au dépôt et à la diffusion de documents scientifiques de niveau recherche, publiés ou non, émanant des établissements d'enseignement et de recherche français ou étrangers, des laboratoires publics ou privés.

## RESEARCH ARTICLE

# Polypeptides derived from $\alpha$ -Synuclein binding partners to prevent $\alpha$ -Synuclein fibrils interaction with and take-up by cells

Elodie Monsellier, Maya Bendifallah, Virginie Redeker, Ronald Melki \*

CEA, Institut François Jacob (MIRcen) and CNRS, Laboratory of Neurodegenerative Diseases (UMR9199), Fontenay-aux-Roses, France

\* [ronald.melki@cnr.fr](mailto:ronald.melki@cnr.fr)

## Abstract

$\alpha$ -Synuclein ( $\alpha$ Syn) fibrils spread from one neuronal cell to another. This prion-like phenomenon is believed to contribute to the progression of the pathology in Parkinson's disease and other synucleinopathies. The binding of  $\alpha$ Syn fibrils originating from affected cells to the plasma membrane of naïve cells is key in their prion-like propagation propensity. To interfere with this process, we designed polypeptides derived from proteins we previously showed to interact with  $\alpha$ Syn fibrils, namely the molecular chaperone Hsc70 and the sodium/potassium pump NaK-ATPase and assessed their capacity to bind  $\alpha$ Syn fibrils and/or interfere with their take-up by cells of neuronal origin. We demonstrate here that polypeptides that coat  $\alpha$ Syn fibrils surfaces in such a way that they are changed affect  $\alpha$ Syn fibrils binding to the plasma membrane components and/or their take-up by cells. Altogether our observations suggest that the rationale design of  $\alpha$ Syn fibrils polypeptide binders that interfere with their propagation between neuronal cells holds therapeutic potential.

## OPEN ACCESS

**Citation:** Monsellier E, Bendifallah M, Redeker V, Melki R (2020) Polypeptides derived from  $\alpha$ -Synuclein binding partners to prevent  $\alpha$ -Synuclein fibrils interaction with and take-up by cells. PLoS ONE 15(8): e0237328. <https://doi.org/10.1371/journal.pone.0237328>

**Editor:** Stephan N. Witt, Louisiana State University Health Sciences Center, UNITED STATES

**Received:** December 20, 2019

**Accepted:** July 23, 2020

**Published:** August 13, 2020

**Peer Review History:** PLOS recognizes the benefits of transparency in the peer review process; therefore, we enable the publication of all of the content of peer review and author responses alongside final, published articles. The editorial history of this article is available here: <https://doi.org/10.1371/journal.pone.0237328>

**Copyright:** © 2020 Monsellier et al. This is an open access article distributed under the terms of the [Creative Commons Attribution License](https://creativecommons.org/licenses/by/4.0/), which permits unrestricted use, distribution, and reproduction in any medium, provided the original author and source are credited.

**Data Availability Statement:** All relevant data are within the manuscript and its Supporting Information files.

## Introduction

The aggregation of proteins into fibrillar high molecular-weight species is involved in human degenerative diseases, including Alzheimer's, Parkinson's, or Huntington's [1]. During the last decade, it has become evident that those protein aggregates traffic between neuronal cells and amplify by seeding the aggregation of their constituting proteins [2–5]. This prion-like phenomenon is thought to be responsible for the stereotypic progression of the pathology in the brain [2,5]. Impeding this phenomenon would be valuable to slow down the progression of disease [6,7].

The spread of amyloid fibrils is a vicious circle involving different steps. First, protein aggregates form with time within neuronal cells [8]. They next escape actively, through export, or passively, upon cell death, the cells where they form [9–12]. The extracellular aggregates dock next to the membrane of naïve neuronal cells [13,14]. This membrane binding steps is followed by the internalization of the fibrils, mainly through endocytosis [15,16]. Once in the cells the aggregates reach the cytoplasm, where they recruit the otherwise soluble endogenous protein they are made of [17], after compromising endo-lysosomal integrity [18].

**Funding:** MB, Région Ile de France through DIM Cerveau et Pensée; RM, Institut de France-Fondation Simone et Cino Del Duca; RM, Fondation Pour La Recherche Médicale (contract DEQ. 20160334896); RM, EC Joint Programme on Neurodegenerative Diseases and Agence Nationale pour la Recherche (TransPathND, ANR-17-JPCD-0002-02 and Protest-70, ANR-17-JPCD-0005-01). Nothing to disclose. The funders had no role in study design, data collection and analysis, decision to publish, or preparation of the manuscript.

**Competing interests:** The authors have declared that no competing interests exist.

**Abbreviations:**  $\alpha$ Syn,  $\alpha$ -Synuclein; NKA, Na<sup>+</sup>/K<sup>+</sup>-ATPase; NBD, Nucleotide Binding Domain; SBD, Substrate Binding Domain; TEV, tobacco etch virus; ThT, Thioflavin T.

Alternatively, they imbalance neuronal proteostasis and trigger the de-novo aggregation of other aggregation prone proteins involved in neurodegenerative diseases [19]. The circle completes when amplified aggregates escape into the extracellular media, targeting new cells.

Every single step of the prion-like propagation process is a potential target for the development of new drugs that would delay the progression of disease. The binding of the extracellular aggregates to the membrane is especially attractive for different reasons [7]. As it takes place in the extracellular environment, it is more easily targetable than intracellular mechanisms [20]. Its underlying molecular mechanisms have been particularly well studied over the past few years [21]. The fibrils bind laterally to the plasma membrane [13]. The binding is mediated by interaction with the plasma membrane lipids [22], with different proteins partners [23–26] and with the extra cellular matrix components [27,28]. The efficiency of the binding depends both on the aggregates characteristics, such as their primary sequence [29,30], their net charge [22], their size [13] or their conformation [17], and on the properties of the membrane, with an emphasis on the role of the membrane curvature [31] and a specific lipid [32] and protein [24,25] composition.

As different membrane components are involved in the interaction with extracellular aggregates in their prion-like propagation process, it seems unlikely that targeting one of them would exert an effect. We therefore decided to target the fibrils themselves, coating them with peptide ligands so that their surface properties are changed and their interaction with membrane partners is compromised. We decided to develop polypeptide binders of fibrils as from a clinical point of view such binders are specific and safe, and their poor pharmacokinetics properties are amenable to optimization [33,34]. Incidentally over 60 peptide drugs have now reached the market [35]. Using a cross-linking and mass spectrometry strategy, we previously mapped the surface interfaces between  $\alpha$ Syn monomers or fibrils and two protein partners, namely, the molecular chaperone Hsc70 [36–38] and the sodium/potassium pump Na<sup>+</sup>/K<sup>+</sup>-ATPase (NKA) [25]. Here, we designed a set of polypeptides based on the Hsc70 and NKA surface areas we identified to interact with  $\alpha$ Syn. We assessed the interaction of the polypeptides derived from Hsc70 and NKA with fibrillar  $\alpha$ Syn in vitro. We identify Hsc70-derived polypeptides that bind best  $\alpha$ Syn fibrils. We also show that an NKA-derived peptide affect fibrils binding to Neuro-2a cells. Overall, our results lay the basis for developing further such polypeptides and improving their affinity for  $\alpha$ Syn fibrils, so that their interactions with and uptake by Neuro-2a neuronal cells are affected.

## Results

### Hsc70 binds to $\alpha$ Syn fibrils with a high affinity, preventing their interaction with the plasma membrane and their take-up by cultured cells

We previously brought evidence for Hsc70 interaction with fibrillar  $\alpha$ Syn using a sedimentation assay [36]. The dissociation constant we measured was 0.1  $\mu$ M. Here we confirmed the interaction between Hsc70 and fibrillar  $\alpha$ Syn using the same sedimentation assay followed by quantitative analysis of the proteins in the pellet and the supernatant fractions by SDS-PAGE (Fig 1A). Hsc70 alone remains in the supernatant, whereas it is pulled into the pellet when incubated for 1h at room temperature with pre-formed  $\alpha$ Syn fibrils. To determine the affinity of Hsc70 for fibrillar  $\alpha$ Syn we incubated preformed  $\alpha$ Syn fibrils (1  $\mu$ M) with increasing amount (0–2  $\mu$ M) of a mix of unlabelled and ATTO488-labeled Hsc70 (labelled:unlabelled molar ratio of 1:50) for 1h at room temperature. The samples were then filtered through cellulose acetate membranes that retains fibrillar  $\alpha$ Syn along with their binders, and the amount of ATTO488-Hsc70 was quantified by fluorescence measurements (Fig 1B). We measured a dissociation constant ( $K_D$ ) between Hsc70-ATTO488 and  $\alpha$ Syn fibrils of  $0.49 \pm 0.02 \mu$ M, consistent with previously published values [36,39]. We demonstrated that the binding between the

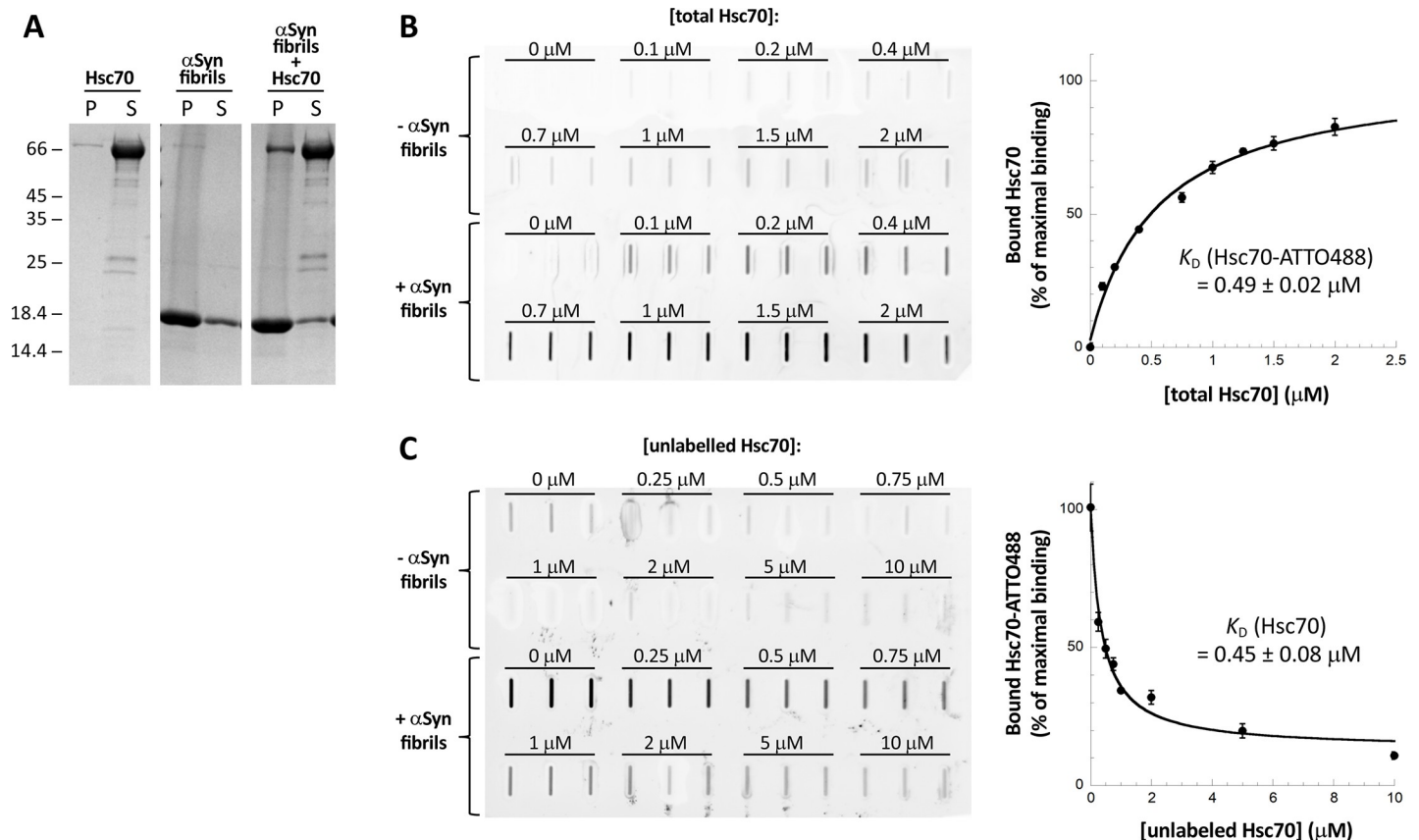


**Fig 1. Hsc70 binds to  $\alpha$ Syn fibrils with high affinity.** A, Hsc70 binds to  $\alpha$ Syn fibrils *in vitro*. SDS-PAGE analysis of the pellet (P) and supernatant (S) fractions of Hsc70 (10  $\mu$ M), fibrillar  $\alpha$ Syn (100  $\mu$ M), and fibrillar  $\alpha$ Syn (100  $\mu$ M) incubated with Hsc70 (10  $\mu$ M) for 1 h at RT. B, Quantification of Hsc70-ATTO488 binding to  $\alpha$ Syn fibrils using the cellulose acetate filter trap assay. Hsc70-ATTO488 was diluted with unlabelled Hsc70 (labelled:unlabelled molar ratio of 1:50) to different final concentrations (0–2  $\mu$ M) and incubated with or without  $\alpha$ Syn fibrils (1  $\mu$ M) for 1 h at RT. Each sample was filtered in triplicate through a cellulose acetate membrane and the amount of Hsc70-ATTO488 trapped onto the membrane was quantified. The mean amount of Hsc70-ATTO488 bound to the  $\alpha$ Syn fibrils normalized to the amount of Hsc70-ATTO488 bound at the maximal concentration used (“% of maximal binding”) and the associated standard error values were calculated from 2 to 3 independent experiments. A filter trap membrane from one representative experiment is shown. C, Unlabelled Hsc70 compete with Hsc70-ATTO488 for binding to  $\alpha$ Syn fibrils. A fixed concentration of Hsc70-ATTO488 (0.2  $\mu$ M) was incubated with increasing concentrations of unlabelled Hsc70 (0–10  $\mu$ M) and with or without  $\alpha$ Syn fibrils (1  $\mu$ M). Each sample was then filtered in triplicate through a cellulose acetate membrane. The mean amount of Hsc70-ATTO488 bound to the  $\alpha$ Syn fibrils and the associated standard error values were calculated from these triplicates.

<https://doi.org/10.1371/journal.pone.0237328.g001>

two partners was not affected by Hsc70 labelling. Indeed, unlabeled Hsc70 competed in a dose-dependent way with the binding of labeled Hsc70 to  $\alpha$ Syn fibrils (Fig 1C), and the  $K_D$  between Hsc70 and  $\alpha$ Syn fibrils was identical to the  $K_D$  between Hsc70-ATTO488 and  $\alpha$ Syn fibrils ( $0.45 \pm 0.08 \mu$ M).

We next assessed the consequences of Hsc70 interaction with  $\alpha$ Syn fibrils on fibrils binding to the cell membrane and subsequent internalization. We set-up two different assays to assess separately  $\alpha$ Syn fibrils binding and internalization (Fig 2). Preformed Alexa488-labeled  $\alpha$ Syn fibrils (S1 Fig) bound to cultured Neuro-2a cells within 30 min incubation in a dose-dependent manner as assessed by quantification of fluorescent foci at cell membranes (Figs 2A and S2A). The addition of Trypan blue quenched all the fluorescence, indicating that the fibrils are located at the plasma membranes. We previously demonstrated that monomeric  $\alpha$ Syn does not bind to cells in such a way [40,41]. This robust cellular binding assay was next used to monitor the effect Hsc70-fibrillar  $\alpha$ Syn interaction on fibrils binding to Neuro-2a cells.  $\alpha$ Syn fibrils (1  $\mu$ M) were pre-incubated with increasing amounts of Hsc70 (0–10  $\mu$ M). Neuro-2a

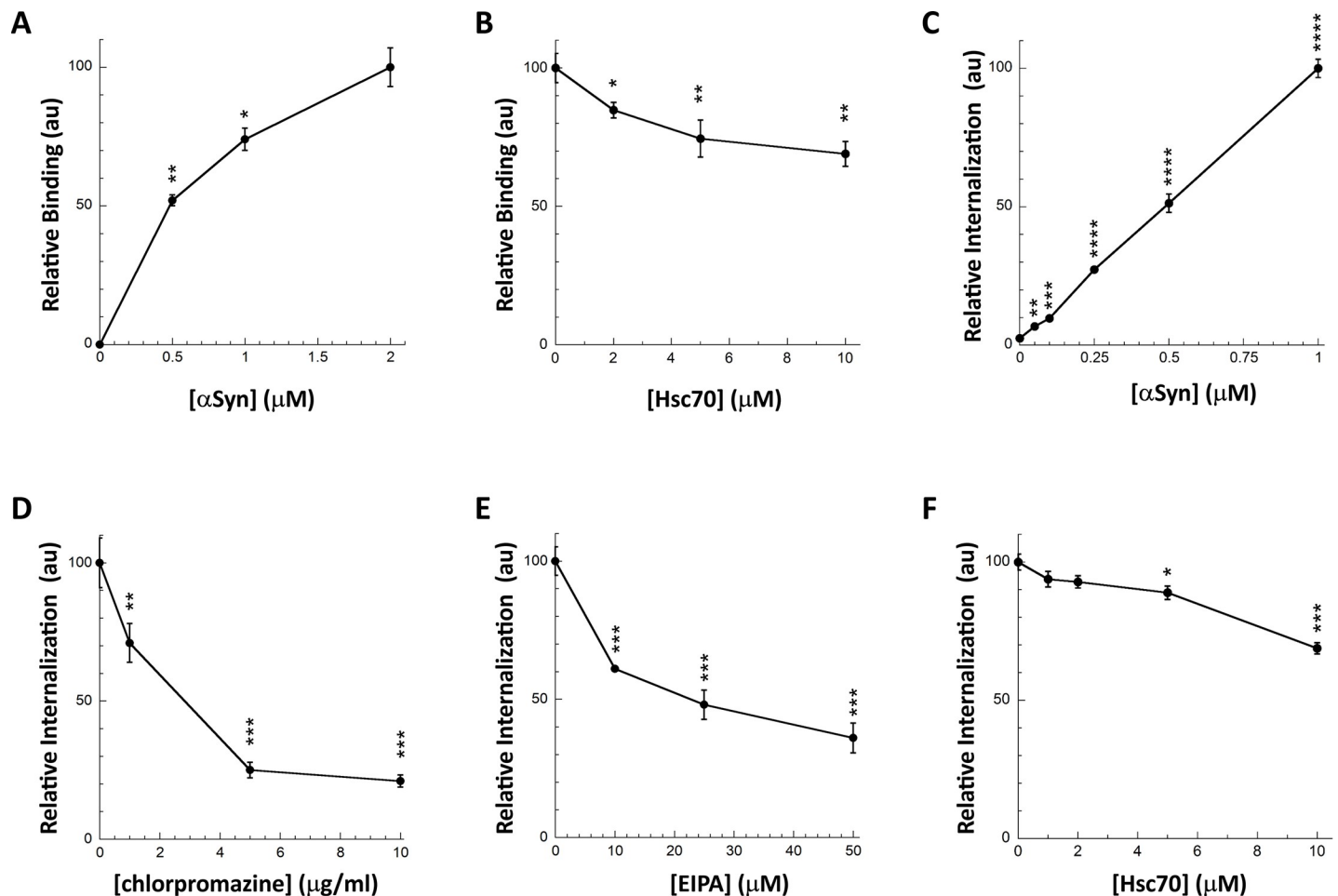


**Fig 2. Hsc70 binding to  $\alpha$ Syn fibrils interferes with their interaction with the plasma membrane and their subsequent internalization.** **A**, Dose-dependent binding of  $\alpha$ Syn fibrils to the plasma membrane of Neuro-2a cells. Neuro-2a cells were exposed for 30 min to  $\alpha$ Syn-Alexa488 fibrils (0–2  $\mu$ M). The cells were extensively washed and the fluorescence quantified. Representative images are shown in **S2A Fig**. For each concentration the mean percentage of Neuro-2a cells bound with at least 1  $\alpha$ Syn-Alexa488 fibrils foci and its associated standard error value was calculated from 3 independent experiments. The results and the associated significances are expressed relative to maximum binding. **B**, Hsc70 prevents  $\alpha$ Syn fibrils binding to the plasma membrane.  $\alpha$ Syn-Alexa488 fibrils (1  $\mu$ M) were incubated with increasing concentrations of Hsc70 (0–10  $\mu$ M) in DMEM for 30 min at 37°C. Neuro-2a cells were next exposed to the mixture for 30 min. Fluorescence was quantified after extensive washing. Representative images are shown in **S2B Fig**. For each Hsc70 concentration, the mean percentage of Neuro-2a cells with at least one  $\alpha$ Syn-Alexa488 fibrils foci and its associated standard error value was calculated from 3 to 5 independent experiments. The results and the associated significances are expressed relative to fibrils binding in the absence of Hsc70. **C**,  $\alpha$ Syn fibrils take-up by Neuro-2a cells. Neuro-2a cells in 96-wells plates were exposed for 4 hours to increasing concentrations of  $\alpha$ Syn-Alexa488 fibrils. Trypan blue was added after extensive washing to quench the fluorescence of plasma membrane-bound  $\alpha$ Syn fibrils. The amount of internalized  $\alpha$ Syn-Alexa488 was measured on a fluorescence plate reader. Means and their associated standard error values were calculated from 5 independent wells. The results are expressed relative to maximum internalization (1  $\mu$ M  $\alpha$ Syn fibrils). Significances are calculated in comparison to the absence of internalization (no  $\alpha$ Syn). **D,E**, Chlorpromazine (**D**) and l’5-N-ethyl-isopropyl-amiloride (EIPA; **E**) prevent  $\alpha$ Syn fibrils internalization by Neuro-2a cells. Neuro-2a cells in 96-wells plates were exposed for 1 hour to increasing concentrations of chlorpromazine (0–10  $\mu$ g/ml) or EIPA (0–50  $\mu$ M) before addition of  $\alpha$ Syn-Alexa488 fibrils (0.5  $\mu$ M). After 4 hours of incubation and extensive washing, Trypan blue was added to quench the fluorescence of plasma membrane-bound  $\alpha$ Syn fibrils. The amount of internalized  $\alpha$ Syn-Alexa488 was measured on a fluorescence plate reader. Means and their associated standard error values were calculated from 5 independent wells. The results and the associated significances are expressed relative to the absence of inhibitors. **F**, Hsc70 prevents  $\alpha$ Syn fibrils internalization by Neuro-2a cells.  $\alpha$ Syn-Alexa488 fibrils (0.5  $\mu$ M) were incubated with increasing concentrations of Hsc70 (0–10  $\mu$ M) in DMEM for 30 min at 37°C. Neuro-2a cells in 96-wells plates were exposed for 4 hours to the mixture. Trypan blue was added after extensive washing to quench the fluorescence of plasma membrane-bound  $\alpha$ Syn fibrils. The amount of internalized  $\alpha$ Syn-Alexa488 was measured on a fluorescence plate reader. Means and their associated standard error values were calculated from 3 independent experiments. The results and the associated significances are expressed relative to internalization in the absence of Hsc70.

<https://doi.org/10.1371/journal.pone.0237328.g002>

cultured cells were then incubated for 30 min with this mix. The data presented in **Figs 2B** and **S2B** clearly demonstrate that Hsc70 affects  $\alpha$ Syn fibrils binding to Neuro-2a cells in a dose-dependent manner.

Fibrillar  $\alpha$ Syn uptake by cells can be assessed quantitatively by fluorescence microscopy after quenching of the fluorescence at cells plasma membrane by Trypan blue (S3 Fig). To increase statistical power we set-up a robust 96-wells plate assay [42]. Neuro-2a cells, in 96-wells plate, were exposed for 4h to Alexa488-labeled  $\alpha$ Syn fibrils pre-incubated with Hsc70 or not, prior to Trypan blue addition and quantification of Alexa488 fluorescence in a plate-reader. The amount of internalized fibrils was determined in a dose- (Fig 2C) and time-dependent manner. Fibrillar  $\alpha$ Syn take-up was inhibited in a dose-dependent manner by chlorpromazine and l'5-N-ethyl-isopropyl-amiloride (EIPA) that inhibits clathrin-mediated endocytosis [43] and macropinocytosis [44], respectively, suggesting that the fibrils are taken up by endocytosis (Fig 2D and 2E). We and others previously demonstrated that endocytically internalized  $\alpha$ Syn fibrils are then able to escape the endocytic pathway and reach the cytosol by endosomal rupture [45–47]. Preincubation of Alexa488-labeled  $\alpha$ Syn fibrils with Hsc70 significantly affected their take-up (Fig 2F). We used Hoechst staining to ascertain that the number of cells remained constant (see Material & Methods).

We conclude from these observations that Hsc70 binding to  $\alpha$ Syn fibrils affects their binding and take-up by neuronal Neuro-2a cells in a dose-dependent manner. The use of full-length Hsc70 for therapeutic purposes has drawbacks because of its pleiotropic effects within cells. We thus aimed at generating fragments of Hsc70 that retain  $\alpha$ Syn fibrils binding capacity.

### Hsc70 Substrate Binding Domain and sub-domains retain $\alpha$ Syn fibrils binding capacity

In a first step toward the design of Hsc70-derived peptides that would potentially retain their ability to bind  $\alpha$ Syn fibrils, we assessed the affinity of different Hsc70 sub-domains for  $\alpha$ Syn fibrils (Figs 3 and 4). Hsc70 is composed of two domains, a Nucleotide Binding Domain (NBD), responsible for the chaperone ATPase activity, and a Substrate Binding Domain (SBD), that binds Hsc70 clients. We previously used lysine-reactive chemical cross-linkers and mass-spectrometry to map the surface areas within Hsc70 that interact with monomeric  $\alpha$ Syn; all the identified areas were within the SBD (Fig 3A) [37,38]. To determine whether Hsc70 SBD retains the ability to bind  $\alpha$ Syn fibrils we expressed and purified it. Hsc70 SBD (Fig 3B, left) can be subdivided in 2 sub-domains, a  $\beta$ -strands/sheet rich (SBD $\beta$ ; Fig 3B, middle) and an  $\alpha$ -helical domain, named “SBD-lid” (Fig 3B, right). Lysine residues from both of these sub-domains are located within the Hsc70- $\alpha$ Syn interaction interface suggesting that they both contribute to  $\alpha$ Syn binding. We therefore expressed and purified SBD $\beta$  and SBD-lid.

The secondary structure content of Hsc70 SBD, SBD $\beta$  and SBD-lid was assessed by circular dichroism measurements. The data suggest that the polypeptide conformation is retained (Figs 3B, 4A and S4A Fig). We next assessed SBD, SBD $\beta$  and SBD-lid binding to  $\alpha$ Syn fibrils as described for full-length Hsc70 and derived dissociation constants from those measurements (Figs 4B and S5 Fig). All three domains bind  $\alpha$ Syn fibrils. Moreover, the  $K_D$  were similar to that we determined for full-length Hsc70 (Fig 4B). Thus, both Hsc70 SBD $\beta$  and SBD-lid contribute to fibrillar  $\alpha$ Syn binding as for monomeric  $\alpha$ Syn [37,38].

### $\alpha$ Syn fibrils Hsc70-derived peptides binders

To identify peptides derived from Hsc70 that have all that is necessary and sufficient to bind  $\alpha$ Syn fibrils, we synthesized ten 11 to 24 residues Hsc70-derived polypeptides (Table 1; Fig 3C) based on the regions that contribute to  $\alpha$ Syn binding and/or participate to the canonical substrate groove (Fig 3A). Some peptides were overlapping to maximise their chances of adopting the right conformation and binding (i.e. Hsc-2 and Hsc-3). Hsc-1, 2, 3, 9 and 10

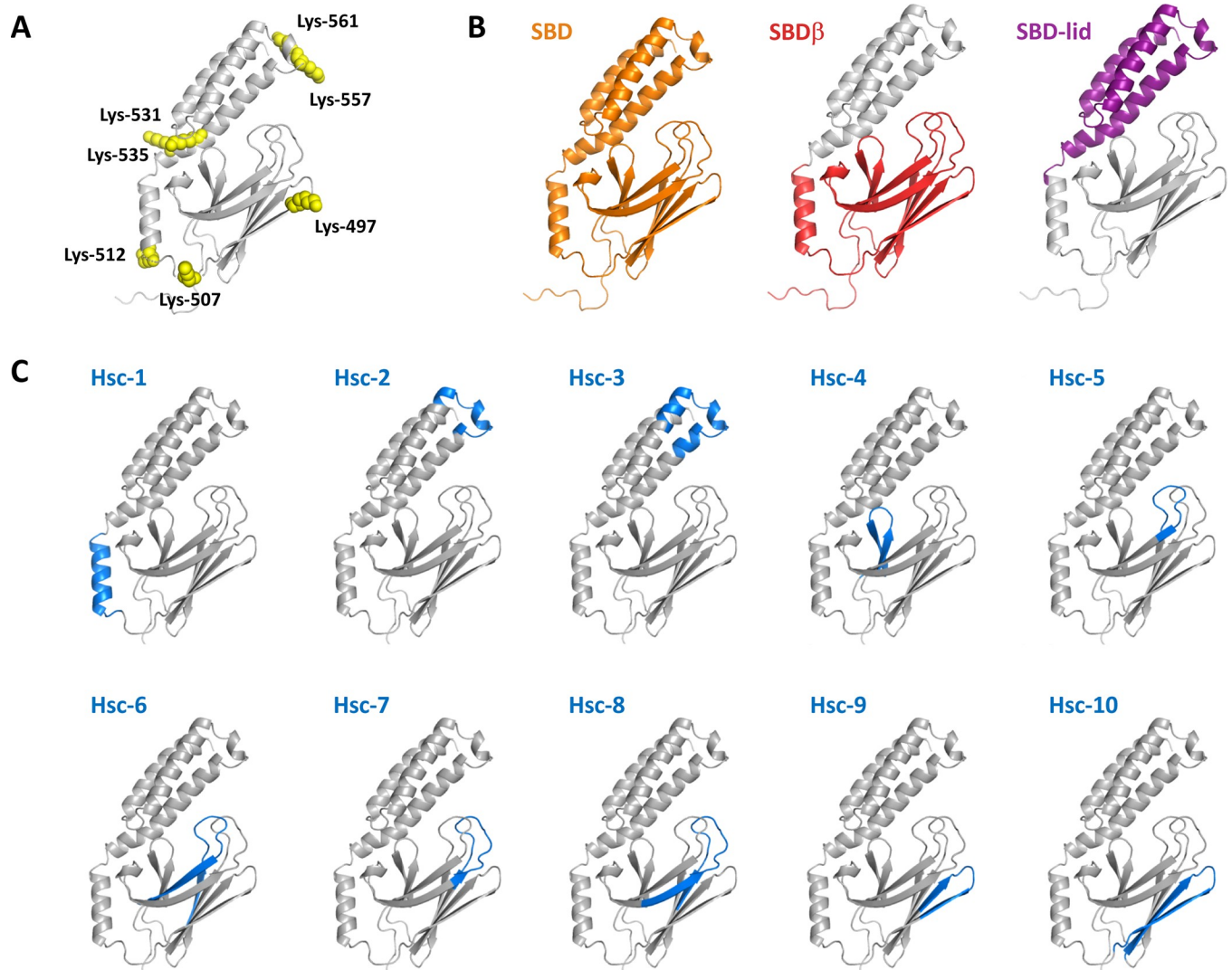


**Fig 3. Hsc70 domains and peptides used throughout this study.** A,  $\alpha$ Syn-binding sites on Hsc70. The binding sites were determined by cross-linking Hsc70 to monomeric  $\alpha$ Syn with chemical cross-linkers and identifying the surface interfaces by mass-spectrometry [37,38]. Only the substrate-binding domain (SBD) of Hsc70 is shown. Cross-linked lysines are depicted in yellow (space fill). Hsc70 model was built as described in [37]. B, Hsc70 SBD sub-domains. SBD  $\beta$ -sandwich (SBD $\beta$ ) and lid (SBD-Lid) sub-domain are coloured. C, Hsc70-derived peptides. 10 peptides, which primary structure is given in Table 1, reproducing Hsc70 amino acid stretches involved in  $\alpha$ Syn binding and the canonical Hsc70 client proteins binding sites [48], were synthesized.

<https://doi.org/10.1371/journal.pone.0237328.g003>

encompass Hsc70- $\alpha$ Syn interaction surface interfaces [37,38]. Hsc-4, 5 and 6 reproduce Hsc70 canonical client binding cavity [40]. Hsc-7 and 8 decal the rest of Hsc70 SBD $\beta$  loops. Hsc-4 and 9 were found insoluble in PBS. Their interaction with  $\alpha$ Syn was not further studied. The secondary structure content of the 8 remaining peptides was assessed by circular dichroism measurements (Table 1 and S4B Fig). The peptides were predominantly unstructured, with the exception of Hsc-1 and 10 (52 and 46%  $\alpha$ -helical, respectively). The presence of an  $\alpha$ -helical conformation in the Hsc-1 peptide is coherent with the structure of this peptide within Hsc70 while Hsc-10 was expected to adopt a hairpin structure (Fig 3C).

Hsc70 binding to monomeric  $\alpha$ Syn affects assembly into fibrils [36]. We therefore first assessed Hsc70-derived peptide capacity to interact with monomeric  $\alpha$ Syn through their ability to affect assembly into fibrils (Fig 5). Monomeric  $\alpha$ Syn assembly into fibrils was monitored

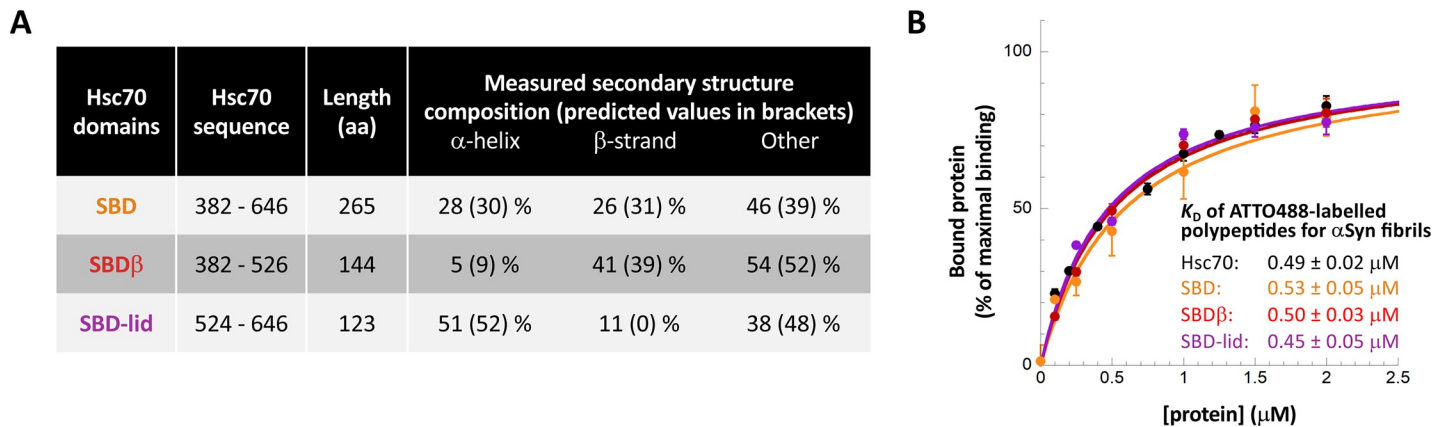


**Fig 4. Hsc70 domains and their binding to  $\alpha$ Syn fibrils.** A, Secondary structure of Hsc70 SBD and sub-domains. The CD spectra used for deconvolution are shown in S4A Fig. B, Determination of Hsc70 domains–  $\alpha$ Syn interactions  $K_D$ . The experiments were performed as in Fig 1B. In each case the normalized mean amount of labelled Hsc70 domain bound to the fibrils (% of maximal binding) and the associated standard error values were calculated from 2 to 3 independent experiments. Representative raw data are shown in S5 Fig.

<https://doi.org/10.1371/journal.pone.0237328.g004>

using Thioflavin T (ThT) binding at 37°C in the absence or the presence of equimolar amounts of each peptide. Hsc-6 significantly slowed down  $\alpha$ Syn assembly into fibrils while Hsc-10 accelerated aggregation (Fig 5A and 5B). The fibrillar nature of the assemblies obtained at the end of the reactions were assessed by transmission electron microscopy (Fig 5C). We conclude from these observations that 2 out of the 8 Hsc70-derived peptides we tested (Hsc-6 and 10) interact with monomeric  $\alpha$ Syn in such a way that the time course of assembly into fibrils is significantly affected.

We next assessed Hsc70-derived peptides binding to fibrillar  $\alpha$ Syn. Fibrillar  $\alpha$ Syn (100  $\mu$ M) was incubated with each peptide (200  $\mu$ M). The fibrils were sedimented and resuspended and the bound Hsc70-derived peptides were quantified by reversed phase chromatography. The results are presented in Table 2 and S6A–S6F Fig. Hsc-1, 2, 3, 5, 7 and 8, did not bind to  $\alpha$ Syn fibrils. Hsc-6 and 10 did bind to the fibrils. As a positive control we used the aromatic molecule Surfen, which is known to bind to the SEVI amyloid fibrils and to prevent their interaction with cells [49]. Surfen was found to bind to  $\alpha$ Syn fibrils (Table 2).

The affinities of Hsc-6 and 10 for  $\alpha$ Syn fibrils were determined and the  $K_D$  were over 100  $\mu$ M (S6G and S6H Fig). Nonetheless, to determine whether Hsc70-derived peptides affect fibrillar  $\alpha$ Syn uptake by cells, Alexa488-labeled  $\alpha$ Syn fibrils were pre-incubated with up to 10

**Table 1. Hsc70-derived peptides primary and secondary structures.** The CD spectra used for deconvolution are shown in S4B Fig.

Peptide	Hsc70 sequence	Sequence	Secondary structure composition		
			$\alpha$ -helix	$\beta$ -strand	other
Hsc-1	510–525	LSKEDIERMVQEAKEY	52%	0%	48%
Hsc-2	553–566	VEDEKLQKINDED	6%	13%	81%
Hsc-3	548–571	NMKATVEDEKLQKINDEDKQKIL	9%	7%	84%
Hsc-4	400–415	SLGIETAGGVMTVLIK			
Hsc-5	428–439	FTTYSNQPVG	0%	15%	85%
Hsc-6	422–444	TKQTQFTTYSNQPVGVLIVYE	0%	20%	80%
Hsc-7	461–475	LTGIPPAPRGVPQIE	10%	17%	73%
Hsc-8	457–477	GKFELTGIPPAPRGVPQIEVT	7%	24%	69%
Hsc-9	489–500	SAVDKSTGKENK			
Hsc-10	484–505	GILNVSVDKSTGKENKITITN	46%	13%	41%

<https://doi.org/10.1371/journal.pone.0237328.t001>

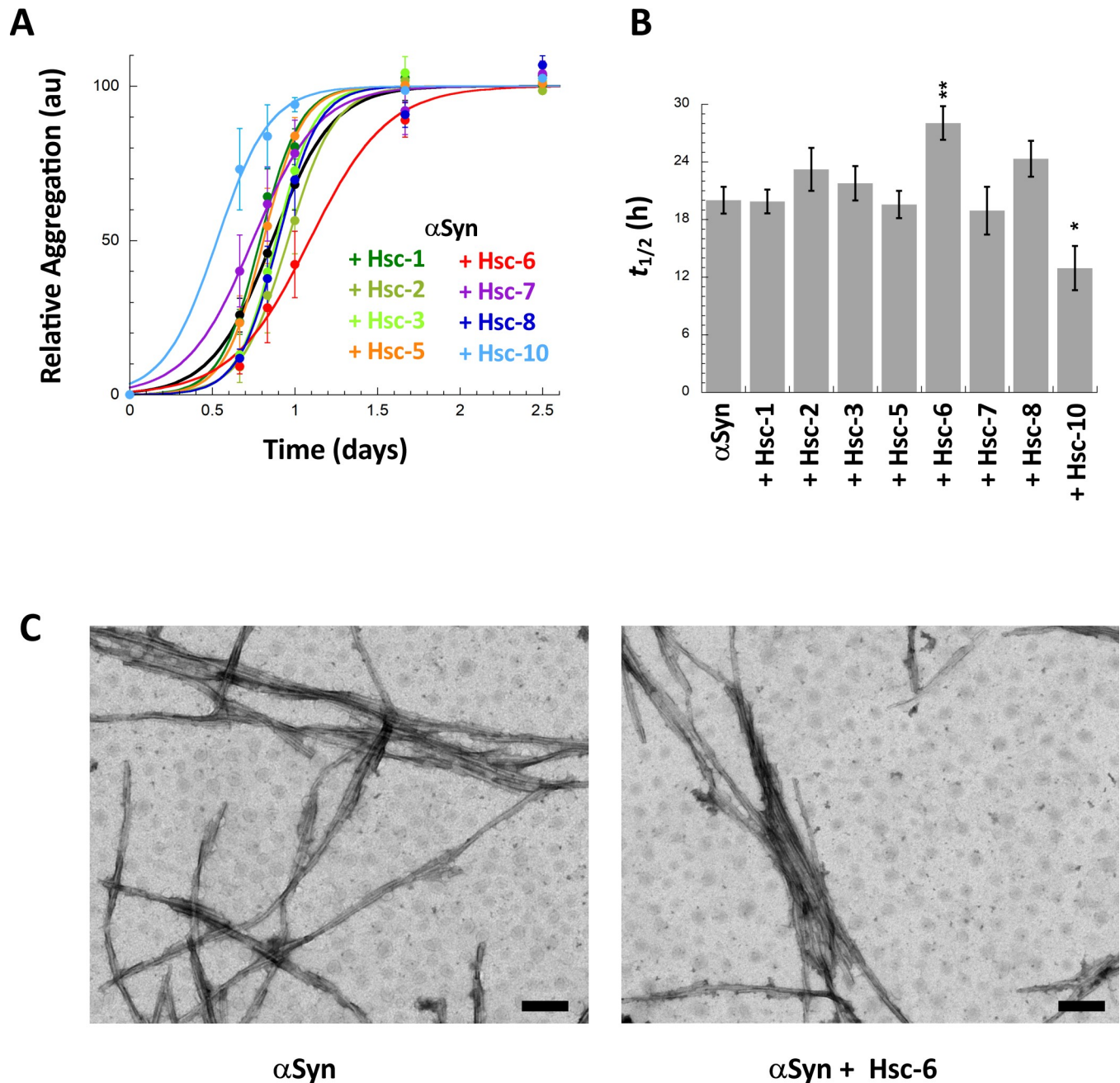


**Fig 5. Effect of Hsc70 SBD-derived peptides on  $\alpha$ Syn aggregation.** **A**, Time-course of  $\alpha$ Syn aggregation in the absence or presence of Hsc70 SBD-derived peptides. Soluble  $\alpha$ Syn (50  $\mu$ M) was incubated with or without Hsc70-derived peptides (50  $\mu$ M) at 37°C and 600 rpm in PBS. The assembly reactions were monitored by Thioflavin T binding. Means and their associated standard errors values were calculated from 4 independent experiments. The lines through the data points represent the best fits to a sigmoid function. **B**, Effect of Hsc70-derived peptides on the half-time ( $t_{1/2}$ ) of  $\alpha$ Syn aggregation. For each independent experiment, the  $t_{1/2}$  parameter was extracted from the best fit to a sigmoid function. The means and their associated standard error values were calculated from 4 independent experiments. **C**, Negative stained electron micrographs of  $\alpha$ Syn assembled alone (left) or in the presence of equimolar concentration of Hsc-6 (right). Scale bar, 200 nm.

<https://doi.org/10.1371/journal.pone.0237328.g005>

molar excess of the different Hsc70-derived peptides and fibrils uptake by Neuro-2a cells was quantified. None of the Hsc70-derived peptides had an effect on  $\alpha$ Syn fibrils take-up (Fig 6). This is consistent with the poor affinity of the best fibrillar  $\alpha$ Syn peptide binders. In contrast,

**Table 2. Binding of the Hsc70-derived peptides to  $\alpha$ Syn fibrils assessed by phase reverse chromatography analysis.**

Sample	Bound $\mu$ M	peptides (%)
Hsc-1	1.2	0.6%
Hsc-2	1.0	0.5%
Hsc-3	1.2	0.6%
Hsc-5	2.8	1.4%
Hsc-6	68	34%
Hsc-7	1.2	0.6%
Hsc-8	1.6	0.8%
Hsc-10	72	36%
Surfen	176	88%

<https://doi.org/10.1371/journal.pone.0237328.t002>

preincubation of  $\alpha$ Syn fibrils with Surfen affected, in a dose-dependent way, their take-up by Neuro-2a cells (Fig 6).

### Peptide derived from an $\alpha$ Syn fibrils membrane partner, the $\alpha$ 3 subunit of the $\text{Na}^+/\text{K}^+$ -ATPase (NKA)

We previously brought evidence for interaction of fibrillar  $\alpha$ Syn with the  $\alpha$ 3-subunit of the membrane ion pump NKA by pull-down [25].  $\alpha$ 3NKA amino acid stretch that interacts with  $\alpha$ Syn was identified by cross-linking and mass spectrometry. It consists of the extracellular loop connecting the transmembrane helices 7 and 8 [25]. Interaction of fibrillar  $\alpha$ Syn with this extracellular loop of  $\alpha$ 3NKA was further confirmed by mutagenesis studies [25]. To determine whether NKA derived peptides affect  $\alpha$ Syn fibrils binding to and take-up by Neuro-2a cells, we synthesized a 27 amino acid residues long peptide (NKApép) that reproduces this loop within  $\alpha$ 3NKA (Fig 7A). NKApép is soluble in PBS; it is disordered with some  $\beta$ -strand content, as assessed by circular dichroism (Figs 7B and S4C).

NKApép neither affected  $\alpha$ Syn aggregation (not shown) nor bound to preformed  $\alpha$ Syn fibrils (S6D and S6F Fig). Preincubation of preformed  $\alpha$ Syn fibrils with NKApép resulted in a dose-dependent reduction in fibrillar  $\alpha$ Syn binding to Neuro-2a cells (Figs 7C and S2C) but did not affect fibrils take-up (Fig 7D). Altogether, although designed to affect fibrillar  $\alpha$ Syn binding to cells, NKApép acts somewhat differently, possibly through interactions with other membranous components.

## Discussion

$\alpha$ Syn fibrils are able to spread from one neuronal cell to another [2–4]. This process is believed to contribute to the spatiotemporal progression of pathology in the central nervous system [2,5]. The binding of  $\alpha$ Syn fibrils to naïve cells, after their formation and release from affected counterparts, is key and has been actively documented as it constitutes a potential target for therapeutic interventions [7,13]. We hypothesized that ligands that change the surface properties of  $\alpha$ Syn fibrils should affect binding to cell membranes. We previously showed that Hsc70 binding to  $\alpha$ Syn fibrils affects the viability of cultured cells of neuronal origin [36]. We demonstrate here that Hsc70 interaction with  $\alpha$ Syn fibrils compromises their binding and take-up by cells. The pleiotropic functions of full-length Hsc70 limit its therapeutic potential [50,51]. We therefore generated polypeptides reproducing Hsc70 sub-domains and surfaces that we previously showed to interact with  $\alpha$ Syn through cross-linking studies [37,38] and assessed their effect on  $\alpha$ Syn fibrils binding to and take-up by cells of neuronal nature. We show here that

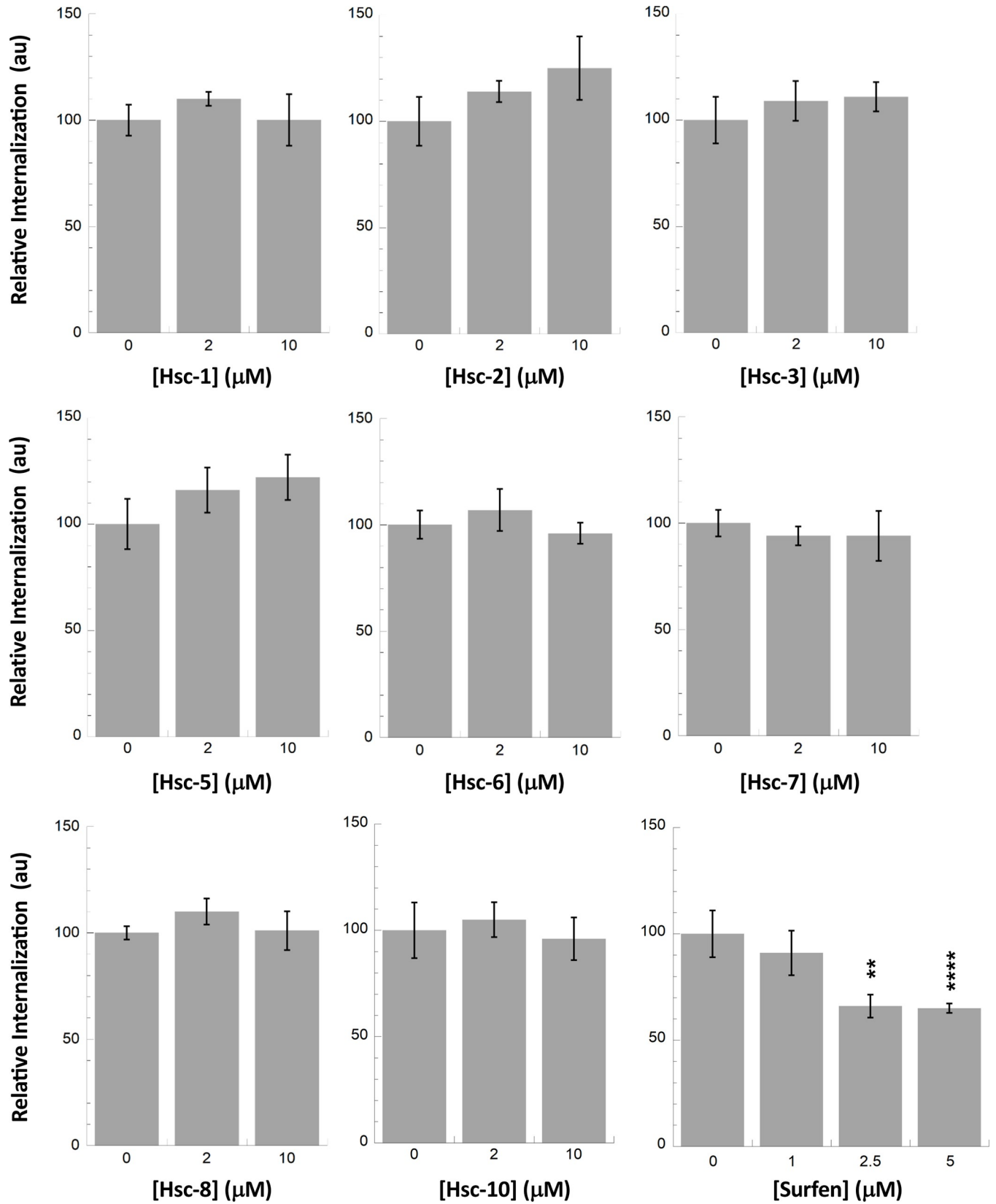


**Fig 6. Effect of Hsc70 SBD-derived peptides on  $\alpha$ Syn fibrils take-up by Neuro-2a cells.** Each Hsc70 SBD-derived peptide (2 or 10  $\mu$ M) was incubated with Alexa488-labeled  $\alpha$ Syn fibrils (1  $\mu$ M) in DMEM for 30 min at 37°C. Neuro-2a cells grown in 96-wells plates were exposed to the mixture for 2 hours. After extensive washing trypan blue was added to quench the fluorescence of plasma membrane-bound  $\alpha$ Syn fibrils. The amount of internalized  $\alpha$ Syn-Alexa488 was measured using a fluorescence plate reader. Means and their associated standard error values were calculated from 3 independent experiments. The same experiment was carried out with Surfen.

<https://doi.org/10.1371/journal.pone.0237328.g006>

two peptides derived from Hsc70 SBD interact with  $\alpha$ Syn without affecting, most probably because of their limited affinity, their take-up by Neuro-2a cells [52,53].

We previously identified through unbiased pull-down and cross-linking strategies a fibrillar  $\alpha$ Syn neuron membrane proteins interactome [25]. Polypeptides reproducing  $\alpha$ Syn protein partners may interfere with fibrils binding to their targets. We therefore assessed the shielding propensity of NKApep, an NKA-derived peptide that encompasses a region we showed to interact with fibrillar  $\alpha$ Syn [25]. NKApep did not bind to  $\alpha$ Syn fibrils under our experimental conditions, nonetheless, we show here that it interferes with fibrillar  $\alpha$ Syn binding to cells. This suggests that NKApep affects  $\alpha$ Syn fibrils binding to the cell indirectly, possibly through the redistribution of other  $\alpha$ Syn fibrils target proteins [21].

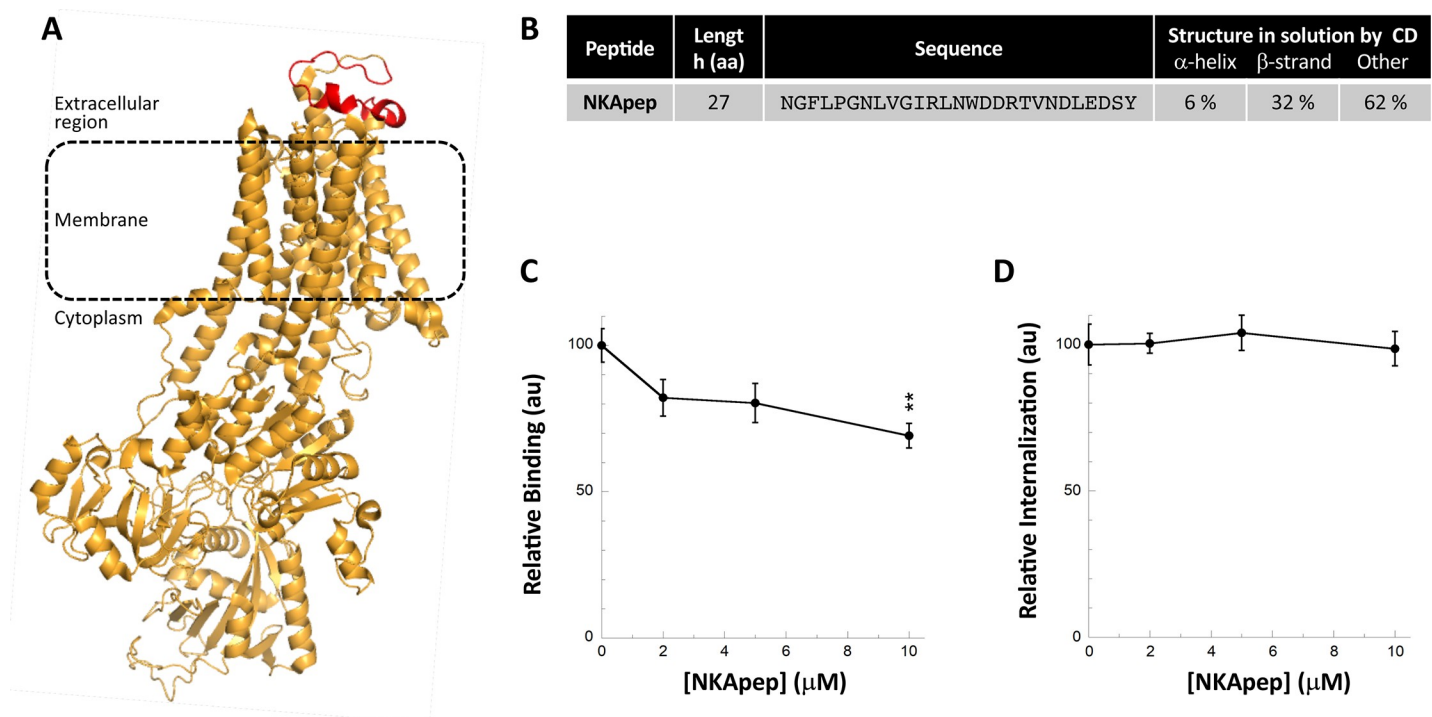


**Fig 7. Effect of a peptide derived from the  $\alpha$ 3 subunit of the NKA on  $\alpha$ Syn fibrils binding and take-up by Neuro-2a cells.** **A**, Structure of the  $\alpha$ 3 subunit of the NKA *Bos taurus* (PDB 4xe5) where the 27 amino acid residues long peptide NKApep corresponding to the extracellular loop previously shown to interact with  $\alpha$ Syn fibrils [25] is coloured in red. **B**, Secondary structure content of NKApep determined by circular dichroism. The CD spectra used for deconvolution is shown in S4C Fig. **C**, Effect of NKApep on  $\alpha$ Syn fibrils binding to the plasma membrane of Neuro-2a cells.  $\alpha$ Syn-Alexa488 fibrils (1  $\mu$ M) were incubated without or with increasing concentrations of NKApep in DMEM for 30 min at 37°C. Neuro-2a cells were next exposed to the mixture for 30 min. Fluorescence was quantified after extensive washing. Representative images are shown in S2B Fig. For each peptide concentration, the mean percentage of Neuro-2a cells with at least 1  $\alpha$ Syn-Alexa488 fibrils foci and its associated standard error value was calculated from 3 independent experiments. The results and the associated significances are expressed relative to fibrils binding in the absence of peptide. **D**, Effect of NKApep on  $\alpha$ Syn fibrils take-up by Neuro-2a cells.  $\alpha$ Syn-Alexa488 fibrils (0.5  $\mu$ M) were incubated with increasing concentrations of NKApep (0–10  $\mu$ M) in DMEM for 30 min at 37°C. Neuro-2a cells grown in 96-wells plates were exposed to the mixture for 4 hours. After extensive washing trypan blue was added to quench the fluorescence of plasma membrane-bound  $\alpha$ Syn fibrils. The amount of internalized  $\alpha$ Syn-Alexa488 was measured using a fluorescence plate reader. Means and their associated standard error values were calculated from 4 independent experiments. The results are expressed relative to the internalization in the absence of peptide.

<https://doi.org/10.1371/journal.pone.0237328.g007>

Overall, our results suggest that polypeptides that bind  $\alpha$ Syn fibrils must have a very high affinity to affect fibrils uptake by cells and hold therapeutic potential. Advantageously, the affinity of polypeptides is amenable to improvements. They can be trimmed and modified by replacing a number of amino acid residues and reassessing affinity in an iterative manner [54]. To limit their folding landscape, they can be stapled using unnatural amino acids bearing alkyl tethers of various lengths at either one or two helix turns [55] or compatible with covalent crosslinking via click chemistry [56], or fused to a scaffolding protein such as thioredoxin [57]. Alternatively, their avidity could be increased by generating tandem repeats of the same or different peptides that bind  $\alpha$ Syn fibrils. Many other modifications can be made so that pharmacokinetic properties of polypeptides that interfere with  $\alpha$ Syn fibril binding and take-up by cells are improved. Thus, such peptide could yield new therapeutic tools to slow down the progression of synucleinopathies and other neurodegenerative diseases.

## Materials and methods

### Expression and purification of $\alpha$ Syn, Hsc70 and Hsc70 subdomains

Recombinant human wild-type  $\alpha$ Syn was purified as described [58]. Recombinant His<sub>6</sub>-tagged Hsc70 was purified as described [36]. The activity of the purified Hsc70 was assessed using a luciferase refolding assay, as described in [36].

Genes encoding the Hsc70 domain and subdomains SBD, SBD $\beta$  and SBD-lid were amplified from the pPRO-EXHTb (Invitrogen) Hsc70 vector [36] and inserted into a pET-M11 vector with an N-terminal 6xHis tag followed by a tobacco etch virus (TEV) protease cleavage site. Recombinant His-tagged proteins were expressed at 37°C in E.coli strain BL21(DE3) (Stratagene, Santa Clara, CA) and purified as follow. Cells were harvested and resuspended in buffer A (30 mM HEPES pH 7.5, 300 mM NaCl, 10% glycerol, 20 mM imidazole). After sonication and centrifugation, lysate supernatants were filtered and loaded onto a 5 mL Talon metal affinity resin column (Clontech, Saint-Germain-en-Laye, France), equilibrated in buffer A. His tagged proteins were eluted with buffer A supplemented with 500 mM imidazole, and then dialysed in PBS. The His tags were cleaved with addition of His-TEV protease, produced using the plasmid pRK1043 (Addgene, Cambridge, MA), at a 1:25 His-TEV:chaperone molar ratio. 100% cleavage, as assessed by SDS-PAGE, was achieved upon incubating the mixtures for 1h at 37°C. The untagged proteins were purified by collecting the flow through of a 5 mL HisTrap FF column.

Proteins concentrations were determined spectrophotometrically using the following extinction coefficients at 280 nm ( $M^{-1}.cm^{-1}$ ): 5960 for  $\alpha$ Syn; 39310 for Hsc70; 12950 for SBD; 2980 for SBD $\beta$ ; and 9970 for SBD-lid. Pure proteins in PBS were filtered through sterile 0.22- $\mu$ m filters, aliquoted and stored at -80°C.

### Synthetic peptides and Surfen

All the peptides we designed were purchased from GL Biochem Ltd. (Shanghai, China). Peptides were dissolved in PBS at 0.5 mM, aliquoted, and stored at -20°C. Surfen (S6951) was purchased from Sigma, dissolved in DMSO at 5 mM, aliquoted, and stored at -20°C.

### Circular dichroism

Far-UV CD spectra were recorded at 20°C using a JASCO J-810 dichrograph equipped with a thermostated cell holder using a 0.01-cm path length quartz cuvette. Each spectrum was the average of 10 acquisitions recorded in the 260–195 nm range with 0.5-nm steps, a bandwidth

of 2 nm, and at a speed of 50 nm/min. All spectra were buffer corrected. The spectra were deconvoluted with the Dichroweb software [59].

### Assembly of $\alpha$ Syn into fibrils and labelling

For fibril formation,  $\alpha$ Syn was incubated at 200  $\mu$ M in PBS at 37°C under continuous shaking in an Eppendorf Thermomixer set at 600 rpm for 2 weeks to allow completion of the aggregation reaction. The completion of the aggregation reaction was monitored by withdrawing an aliquot (100  $\mu$ L), subjecting it to centrifugation in a 5415R tabletop centrifuge (Eppendorf) at 20,000g and 20°C for 30 min and assessing spectrophotometrically the amount of  $\alpha$ Syn remaining in the supernatant. The proportion of soluble  $\alpha$ Syn was systematically less than 10% (S1A Fig). The fibrillar nature of the aggregates obtained at the end of the aggregation reaction (S1B Fig) was assessed using a Jeol 1400 transmission electron microscope (Jeol Ltd.) following adsorption of the samples onto carbon-coated 200-mesh grids and negative staining with 1% uranyl acetate. The images were recorded with a Gatan Orius CCD camera (Gatan).

For cellular binding and internalization experiments, the fibrils were labeled by addition of the aminoreactive fluorescent dye Alexa 488 (Invitrogen, Carlsbad, CA, USA) using a protein:dye molar ratio of 10:1 based on initial monomer concentration. Labelling was performed following the manufacturer's recommendation. The reaction was stopped by adding Tris-HCl pH 7.5 (20 mM final concentration). Finally, the fibrils were sonicated with an ultrasound sonicator (Hielscher Ultrasonic, Teltow, Germany) set at an amplitude of 75 and 0.5 s cycles for 1 min.

### Binding of Hsc70, SBD, SBD $\beta$ and SBD-lid to preformed $\alpha$ Syn fibrils and $K_D$ determination

For binding assay,  $\alpha$ Syn fibrils (100  $\mu$ M) alone, Hsc70 alone (10  $\mu$ M) or  $\alpha$ Syn fibrils and Hsc70 (100 and 10  $\mu$ M, respectively) were incubated for 1h at RT in PBS. Samples were spun for 30 min at 50,000g and 20°C in a TL100 tabletop ultracentrifuge (Beckman) and the proportion of Hsc70 present in the pellet vs the supernatant was analysed by SDS-PAGE.

The  $K_D$  for Hsc70, SBD, SBD $\beta$  and SBD-lid interaction with  $\alpha$ Syn fibrils were measured as follow. Hsc70 and its subdomains were first labeled by addition of the aminoreactive fluorescent dye ATTO488 (Invitrogen, Carlsbad, CA, USA) using a protein:dye molar ratio of 1:5. The reaction was stopped by adding Tris-HCl pH 7.5 (20 mM final concentration). The unreacted fluorophore was removed by NAP5 desalting column. Under these conditions the majority of primary amines unaffected by the labelling as 0.05 to 0.08 dye molecules were incorporated on average within Hsc70 or its subdomains, as assessed by absorbance spectroscopy. Binding of ATTO488-labeled polypeptides to fibrillar  $\alpha$ Syn was then followed by a filter retardation assay where fibrils and associated proteins are retained on a membrane [60]. The different ATTO488-labeled polypeptides were diluted with their unlabeled counterpart (labeled:unlabeled polypeptides ratio of 1:50) at different final concentrations (0–2  $\mu$ M) and incubated with or without  $\alpha$ Syn fibrils (1  $\mu$ M) in PBS for 1h at RT. 200  $\mu$ l of each sample were filtered in triplicate through cellulose acetate membranes (0.2  $\mu$ m pore size, Millipore Corp., Bedford, MA) using a 48-slot slot-blot filtration apparatus (GE Healthcare). The amount of labeled polypeptide retained on the membrane was visualized using a ChemiDoc<sup>TM</sup> MP (BioRad). Images were processed and quantified using Image Lab.

Alternatively, to ensure that the labelling did not affect the binding properties of Hsc70 to  $\alpha$ Syn fibrils, a fixed concentration of Hsc70-ATTO488 (0.2  $\mu$ M) was incubated with increasing concentrations of unlabeled Hsc70 (0–10  $\mu$ M) and with or without  $\alpha$ Syn fibrils (1  $\mu$ M) in PBS for 1h at RT. The experiment was then performed as above.

### Assessment of synthetic peptides effect on $\alpha$ Syn assembly

$\alpha$ Syn (50  $\mu$ M monomer concentration) was incubated in the absence or in the presence of peptides (50  $\mu$ M) in PBS at 37°C under continuous shaking in an Eppendorf Thermomixer set at 600 rpm. Aliquots (10  $\mu$ L) were withdrawn at different time intervals from the assembly reaction and mixed to a Thioflavin T solution (10  $\mu$ M; 400  $\mu$ L). Thioflavin T fluorescence was recorded with a Cary Eclipse spectrofluorimeter (Varian Medical Systems Inc.) using excitation and emission wavelengths set at 440 and 480 nm, respectively. The nature of the fibrils obtained at the end of the aggregation reaction was assessed by electron microscopy as described above. The proportion of  $\alpha$ Syn assembled into fibrils was assessed by ultracentrifugation in a TL100 tabletop centrifuge (Beckman) at 50,000g and 20°C for 30 min and analyse of the supernatant and pellet fractions by SDS-PAGE. Following Coomassie staining / destaining the gels were visualized using a ChemiDoc™ MP (BioRad). Images were processed and quantified using Image Lab.

### Binding of peptides derived from Hsc70 and NKA and Surfen to preformed $\alpha$ Syn fibrils and $K_D$ determination

Hsc70-derived peptides, the NKApep peptide or the Surfen molecule (0 or 200  $\mu$ M) were incubated with or without  $\alpha$ Syn fibrils (100  $\mu$ M) for 1h at RT in PBS. The samples were centrifuged for 30 min in a 5415R tabletop centrifuge (Eppendorf) at 20,000g and 20°C. The pellets were first washed by 100  $\mu$ L of 0.1% TFA and then dissolved for 30 min in 30  $\mu$ L of pure TFA. After TFA evaporation, the samples were resuspended in 0.1% TFA and stored at -20°C. The composition of each sample was assessed by phase reverse chromatography on a C18 column (Jupiter C18 300A from Phenomenex, Torrance, CA, USA). The solvent composition was 0.1% TFA for solvent A and 80% acetonitrile, 0.09% TFA for solvent B, and the flow was set at 200  $\mu$ L/min. The column was equilibrated in 5% B. The peptides were eluted by a gradient from 5% to 80% of solvent B. The amount of  $\alpha$ Syn-associated ligand present in each sample was determined by comparing their respective absorbance at 215 nm (peptides) or 260 nm (Surfen) to the absorbance of a known amount of the same ligand. For  $K_D$  measurements the same experiment was performed using a range of peptide concentrations (0–200  $\mu$ M).

### Cell culture

Murine neuroblastoma Neuro-2a cells (ATCC, Manassas, VA) were culture at 37°C in humidified air with 5% CO<sub>2</sub> in Dulbecco's modified Eagle's medium (DMEM) containing 10% foetal bovine serum, 2 mM glutamine, 100 units.ml<sup>-1</sup> penicillin and 100  $\mu$ g.ml<sup>-1</sup> streptomycin. All materials used for cell culture were from PAA Laboratories GmbH (Pasching, Austria).

### Binding of $\alpha$ Syn fibrils to Neuro-2a cells

Alexa488-labeled  $\alpha$ Syn fibrils (1  $\mu$ M equivalent monomer concentration) were first incubated for 30 min at 37°C in DMEM without or with the ligands (Hsc70 or the NKApep peptide) at different concentrations. Neuro-2a cells cultured on ibidi- $\mu$ -Dishes (ibidi, Martinsried, Germany) were then incubated for 30 min with this mix. Then, the cells were washed and immediately imaged in serum-free, phenol red-free DMEM on a Zeiss Axio Observer Z1 epifluorescence microscope equipped with an Incubator XLmulti S2 RED LS (Carl Zeiss) and an Orca-R2 camera (Hamamatsu) at a 20x magnification. The percentage of cells with bound Alexa488 foci was estimated by randomly counting at least 500 cells in 10–15 fields and the experiments were reproduced independently 3 times. For each field the number of foci was automatically assessed using the software Fiji [61,62] and an in-house built plugin.

## Internalization of $\alpha$ Syn fibrils by Neuro-2a cells

Neuro-2a cells cultured on ibidi- $\mu$ -Dishes (ibidi, Martinsried, Germany) were exposed for 4h to Alexa488-labeled  $\alpha$ Syn fibrils (1  $\mu$ M equivalent monomer concentration) at 37°C in DMEM. The cells were washed twice with serum-free, phenol red-free DMEM and 0.1% Trypan Blue (Sigma-Aldrich) was added to quench Alexa488 fluorescence at the plasma membrane. The cells were then imaged and the percentage of cells with internalized Alexa488 foci was estimated as described above.

The uptake of Alexa488-labeled  $\alpha$ Syn fibrils (0.5  $\mu$ M equivalent monomer concentration) pre-incubated or not for 30 min at 37°C in DMEM with the ligands (Hsc70, peptides or Surfen) at different concentrations to Neuro-2A cells was also assessed using a 96-well plate assay. The cells cultured on 96-wells plates were incubated with the fibrils, preincubated or not with the ligands for 30 min at 37°C in DMEM, in 5 independent wells. After 4 hours the media was removed and Hoechst (Sigma-Aldrich) diluted at 0.2  $\mu$ g/ml in serum-free, phenol red-free DMEM was added for 30 min. The cells were washed twice with serum-free, phenol red-free DMEM and 0.1% Trypan Blue (Sigma-Aldrich) was added to quench the fluorescence of plasma membrane-bound Alexa488-labeled  $\alpha$ Syn fibrils. For each wells Alexa488 and Hoechst fluorescences were recorded on a Clariostar microplate reader (BMG LABTECH GmbH, Germany). For each condition Alexa488 fluorescence value was considered and averaged over the 5 wells only if the Hoescht value was not significantly different from the one of untreated cells.

To assess to role of endocytosis in  $\alpha$ Syn fibrils internalization, Neuro-2a cells cultured on 96-wells plates were first incubated with increasing concentrations of chlorpromazine or l'5-N-ethyl-isopropyl-amiloride (EIPA). After 1 hour Alexa488-labeled  $\alpha$ Syn fibrils (0.5  $\mu$ M equivalent monomer concentration) was added. The experiment was then performed as above.

## Statistical significance

Statistical significance was determined through an unpaired student's t-test. Annotations used throughout the manuscript to indicate level of significance are as follows: \*  $p < 0.05$ ; \*\*  $p < 0.01$ ; \*\*\*  $p < 0.001$ ; \*\*\*\*  $p < 0.0001$ .

## Supporting information

**S1 Fig.  $\alpha$ Syn fibrils used for the binding and internalization studies.** Monomeric  $\alpha$ Syn was assembled for 2 weeks at 200  $\mu$ M (equivalent monomer concentration), labelled with Alexa488 and sonicated for 1 min, as described in Material & Methods. **A**, The completion of the aggregation reaction was assessed by measuring the concentration of  $\alpha$ Syn in the supernatant at  $t = 0$  and  $t = 2$  weeks. The mean and associated standard deviation values were calculated from 5 independent experiments. **B**, The fibrillar nature of the resulting aggregates assessed by transmission electron microscopy after negative staining. Scale bar, 200 nm. (PDF)

**S2 Fig. Representative epifluorescence and phase contrast images for the binding of  $\alpha$ Syn fibrils to Neuro-2a cells.** **A**, Dose-dependent binding of  $\alpha$ Syn fibrils to the plasma membrane of Neuro-2a cells. Neuro-2a cells were imaged after exposure for 30 min to  $\alpha$ Syn-Alexa488 fibrils (0–2  $\mu$ M equivalent monomer concentration) and extensive washing. **B**,  $\alpha$ Syn fibrils binding to the plasma membrane of Neuro-2a cells in the presence or the absence of Hsp70 and NKApep.  $\alpha$ Syn-Alexa488 fibrils (1  $\mu$ M equivalent monomer concentration) were incubated in the absence (top pannels) or in the presence of Hsc70 (10  $\mu$ M; middle panels) or NKApep (10  $\mu$ M; bottom panels) in DMEM for 30 min at 37°C. Neuro-2a cells were imaged

after exposure to the mixture for 30 min and extensive washing. Scale bars, 20  $\mu$ M.  
(PDF)

**S3 Fig. Internalization of  $\alpha$ Syn fibrils assessed by fluorescence microscopy.** Neuro-2a cells were exposed for 4 hours to  $\alpha$ Syn-Alexa488 fibrils (1  $\mu$ M equivalent monomer concentration). The cells were washed twice with serum-free, phenol red-free DMEM then 0.1% Trypan Blue was added to quench the fluorescence of plasma membrane-bound Alexa488-labeled  $\alpha$ Syn fibrils. Scale bars, 20  $\mu$ M.  
(PDF)

**S4 Fig. CD spectra of domains and peptides used throughout this study.** A, Hsc70 domains SBD, SBD $\beta$  and SBD-lid. B, Hsc70 peptides. C, NKApep.  
(PDF)

**S5 Fig.** Quantification of SBD-ATTO488 (A), SBD $\beta$ -ATTO488 (B) and SBD-lid-ATTO488 (C) binding to  $\alpha$ Syn fibrils. ATTO488-labelled Hsc70 SBD domain and sub-domains were diluted with the corresponding unlabelled proteins (at a molar ratio 1:50) to different final concentrations (0–5  $\mu$ M) and incubated with or without  $\alpha$ Syn fibrils (1  $\mu$ M) for 1h at RT. Each sample was then filtered in triplicate through a cellulose acetate membrane and the amount of ATTO488-labelled Hsc70 domain trapped onto the membrane was quantified. In each case a representative experiment is shown.  $K_D$  values presented in Fig 4B were derived from 2 to 3 independent experiments.  
(PDF)

**S6 Fig. Binding of the peptides Hsc-6, Hsc-7, Hsc-10 and NKApep to  $\alpha$ Syn fibrils and  $K_D$  determination.** A-F,  $\alpha$ Syn fibrils alone (100  $\mu$ M),  $\alpha$ Syn fibrils (100  $\mu$ M) and peptides (200  $\mu$ M) (panels A-D) and Peptides alone (100  $\mu$ M; panels E and F), were incubated 1h at RT. The samples were centrifuged for 30 min at 20.000g and 20°C. The pellets were dissolved in TFA 100%. After evaporation, the samples were resuspended in TFA 0.1%, and analysed by reversed phase chromatography on a C18 column. The retention time of each peptide was determined by a separate injection of 1 nmole of the peptide and is indicated by an arrow; for Hsc-7 (B) and NKApep (D), the arrow indicating the putative position of the peptide is in dotted line since no peptide was found to be associated with the  $\alpha$ Syn pellet. Hsc-6 and Hsc-10 co-sediment with  $\alpha$ Syn fibrils, whereas Hsc-7 and NKApep do not. G, H, Determination of Hsc-6 and Hsc-10 -  $\alpha$ Syn fibrils  $K_D$ . Measurements as described above were performed for increasing peptide concentrations (0–200  $\mu$ M). The amount of  $\alpha$ Syn fibrils-bound Hsc-6 and Hsc-10 is plotted against the total peptide concentration. The lines through the data points represent the best fits to a linear function and are drawn for visual guidance only.  
(PDF)

**S1 Raw images.**  
(PDF)

## Acknowledgments

We thank Mrs Tracy Bellande for expert technical assistance. This work was supported by the Centre National de la Recherche Scientifique, the Institut National de la Santé et de la Recherche Médicale, the Région Ile de France through DIM Cerveau et Pensée, the Institut de France-Fondation Simone et Cino Del Duca, the Fondation Pour La Recherche Médicale (contract DEQ. 20160334896), the EC Joint Programme on Neurodegenerative Diseases and Agence Nationale pour la Recherche (TransPathND, ANR-17-JPCD-0002-02 and Protest-70, ANR-17-JPCD-0005-01). This work benefited from the electron microscopy facility Imagerie-Gif.

## Author Contributions

**Conceptualization:** Elodie Monsellier, Ronald Melki.

**Data curation:** Elodie Monsellier, Maya Bendifallah, Virginie Redeker.

**Formal analysis:** Elodie Monsellier, Maya Bendifallah, Virginie Redeker, Ronald Melki.

**Funding acquisition:** Ronald Melki.

**Investigation:** Elodie Monsellier, Maya Bendifallah, Virginie Redeker, Ronald Melki.

**Methodology:** Ronald Melki.

**Project administration:** Ronald Melki.

**Resources:** Ronald Melki.

**Supervision:** Ronald Melki.

**Writing – original draft:** Elodie Monsellier, Ronald Melki.

## References

1. Knowles TPJ, Vendruscolo M, Dobson CM. The amyloid state and its association with protein misfolding diseases. *Nat Rev Mol Cell Biol.* 2014; 15: 384–396. <https://doi.org/10.1038/nrm3810> PMID: 24854788
2. Brundin P, Melki R, Kopito R. Prion-like transmission of protein aggregates in neurodegenerative diseases. *Nat Rev Mol Cell Biol.* 2010; 11: 301–307. <https://doi.org/10.1038/nrm2873> PMID: 20308987
3. Brundin P, Melki R. Prying into the Prion Hypothesis for Parkinson's Disease. *J Neurosci.* 2017; 37: 9808–9818. <https://doi.org/10.1523/JNEUROSCI.1788-16.2017> PMID: 29021298
4. Vargas JY, Grudina C, Zurzolo C. The prion-like spreading of  $\alpha$ -synuclein: From in vitro to in vivo models of Parkinson's disease. *Ageing Res Rev.* 2019; 50: 89–101. <https://doi.org/10.1016/j.arr.2019.01.012> PMID: 30690184
5. Jucker M, Walker LC. Propagation and spread of pathogenic protein assemblies in neurodegenerative diseases. *Nat Neurosci.* 2018; 21: 1341–1349. <https://doi.org/10.1038/s41593-018-0238-6> PMID: 30258241
6. Eisele YS, Monteiro C, Fearn C, Encalada SE, Wiseman RL, Powers ET, et al. Targeting protein aggregation for the treatment of degenerative diseases. *Nat Rev Drug Discov.* 2015; 14: 759–780. <https://doi.org/10.1038/nrd4593> PMID: 26338154
7. Pemberton S, Melki R. The interaction of Hsc70 protein with fibrillar  $\alpha$ Synuclein and its therapeutic potential in Parkinson disease. *Commun Integr Biol.* 2012; 5: 94–95. <https://doi.org/10.4161/cib.18483> PMID: 22482021
8. Xilouri M, Brekk OR, Stefanis L.  $\alpha$ -Synuclein and protein degradation systems: a reciprocal relationship. *Mol Neurobiol.* 2013; 47: 537–551. <https://doi.org/10.1007/s12035-012-8341-2> PMID: 22941029
9. Abounit S, Bousset L, Loria F, Zhu S, de Chaumont F, Pieri L, et al. Tunneling nanotubes spread fibrillar  $\alpha$ -synuclein by intercellular trafficking of lysosomes. *EMBO J.* 2016; 35: 2120–2138. <https://doi.org/10.15252/embj.201593411> PMID: 27550960
10. Deng J, Koutras C, Donnelier J, Alshehri M, Fotouhi M, Girard M, et al. Neurons Export Extracellular Vesicles Enriched in Cysteine String Protein and Misfolded Protein Cargo. *Sci Rep.* 2017; 7: 956. <https://doi.org/10.1038/s41598-017-01115-6> PMID: 28424476
11. Katsinelos T, Zeitler M, Dimou E, Karakatsani A, Müller HM, Nachman E, et al. Unconventional Secretion Mediates the Trans-cellular Spreading of Tau. *Cell Rep.* 2018; 23: 2039–2055. <https://doi.org/10.1016/j.celrep.2018.04.056> PMID: 29768203
12. Ren PH, Lauckner JE, Kachirskaja I, Heuser JE, Melki R, Kopito RR. Cytoplasmic penetration and persistent infection of mammalian cells by polyglutamine aggregates. *Nat Cell Biol.* 2009; 11: 219–225. <https://doi.org/10.1038/ncb1830> PMID: 19151706
13. Monsellier E, Bousset L, Melki R.  $\alpha$ -Synuclein and huntingtin exon 1 amyloid fibrils bind laterally to the cellular membrane. *Sci Rep.* 2016; 6: 19180. <https://doi.org/10.1038/srep19180> PMID: 26757959
14. Han S, Kollmer M, Markx D, Claus S, Walther P, Fändrich M. Amyloid plaque structure and cell surface interactions of  $\beta$ -amyloid fibrils revealed by electron tomography. *Sci Rep.* 2017; 7: 43577. <https://doi.org/10.1038/srep43577> PMID: 28240273

15. Angot E, Steiner JA, Tomé CM, Ekström P, Mattsson B, Björklund A, et al. Alpha-synuclein cell-to-cell transfer and seeding in grafted dopaminergic neurons in vivo. *PLoS One*. 2012; 7: e39465. <https://doi.org/10.1371/journal.pone.0039465> PMID: 22737239
16. Münch C, O'Brien J, Bertolotti A. Prion-like propagation of mutant superoxide dismutase-1 misfolding in neuronal cells. *Proc Natl Acad Sci*. 2011; 108: 3548–3553. <https://doi.org/10.1073/pnas.1017275108> PMID: 21321227
17. Bousset L, Pieri L, Ruiz-Arlandis G, Gath J, Jensen PH, Habenstein B, et al. Structural and functional characterization of two alpha-synuclein strains. *Nat Commun*. 2013; 4: 2575. <https://doi.org/10.1038/ncomms3575> PMID: 24108358
18. Flavin WP, Bousset L, Green ZC, Chu Y, Skarpathiotis S, Chaney MJ, et al. Endocytic vesicle rupture is a conserved mechanism of cellular invasion by amyloid proteins. *Acta Neuropathol*. 2017; 134: 629–653. <https://doi.org/10.1007/s00401-017-1722-x> PMID: 28527044
19. Gidalevitz T, Ben-Zvi A, Ho KH, Brignull HR, Morimoto RI. Progressive disruption of cellular protein folding in models of polyglutamine diseases. *Science (80-)*. 2006; 311: 1471–1474. <https://doi.org/10.1126/science.1124514> PMID: 16469881
20. Holmes BB, Diamond MI. Prion-like properties of Tau protein: The importance of extracellular Tau as a therapeutic target. *J Biol Chem*. 2014; 289: 19855–19861. <https://doi.org/10.1074/jbc.R114.549295> PMID: 24860099
21. Shrivastava AN, Aperia A, Melki R, Triller A. Physico-Pathologic Mechanisms Involved in Neurodegeneration: Misfolded Protein-Plasma Membrane Interactions. *Neuron*. 2017; 95: 33–50. <https://doi.org/10.1016/j.neuron.2017.05.026> PMID: 28683268
22. Trevino RS, Lauckner JE, Sourigues Y, Pearce MM, Bousset L, Melki R, et al. Fibrillar structure and charge determine the interaction of polyglutamine protein aggregates with the cell surface. *J Biol Chem*. 2012; 287: 29722–29728. <https://doi.org/10.1074/jbc.M112.372474> PMID: 22753412
23. Hamilton A, Zamponi GW, Ferguson SSG. Glutamate receptors function as scaffolds for the regulation of  $\beta$ -amyloid and cellular prion protein signaling complexes. *Mol Brain*. 2015; 8: 18. <https://doi.org/10.1186/s13041-015-0107-0> PMID: 25888324
24. Shrivastava AN, Redeker V, Pieri L, Bousset L, Renner M, Madiona K, et al. Clustering of Tau fibrils impairs the synaptic composition of  $\alpha$ 3-Na<sup>+</sup>/K<sup>+</sup>-ATPase and AMPA receptors. *EMBO J*. 2019; 38: e99871. <https://doi.org/10.15252/embj.201899871> PMID: 30630857
25. Shrivastava AN, Redeker V, Fritz N, Pieri L, Almeida LG, Spolidoro M, et al.  $\alpha$ -synuclein assemblies sequester neuronal  $\alpha$ 3-Na<sup>+</sup>/K<sup>+</sup>-ATPase and impair Na<sup>+</sup> gradient. *EMBO J*. 2015; 34: 2408–2423. <https://doi.org/10.15252/embj.201591397> PMID: 26323479
26. Mao X, Ou MT, Karuppagounder SS, Kam TI, Yin X, Xiong Y, et al. Pathological  $\alpha$ -synuclein transmission initiated by binding lymphocyte-activation gene 3. *Science (80-)*. 2016; 353: aah3374. <https://doi.org/10.1126/science.aah3374> PMID: 27708076
27. Holmes BB, DeVos SL, Kfoury N, Li M, Jacks R, Yanamandra K, et al. Heparan sulfate proteoglycans mediate internalization and propagation of specific proteopathic seeds. *Proc Natl Acad Sci*. 2013; 110: E3138–E3147. <https://doi.org/10.1073/pnas.1301440110> PMID: 23898162
28. Jacob RS, George E, Singh PK, Salot S, Anoop A, Jha NN, et al. Cell adhesion on amyloid fibrils lacking integrin recognition motif. *J Biol Chem*. 2016; 291: 5278–5298. <https://doi.org/10.1074/jbc.M115.678177> PMID: 26742841
29. Kegel KB, Sapp E, Alexander J, Valencia A, Reeves P, Li X, et al. Polyglutamine expansion in huntingtin alters its interaction with phospholipids. *J Neurochem*. 2009; 110: 1585–1597. <https://doi.org/10.1111/j.1471-4159.2009.06255.x> PMID: 19566678
30. Burke KA, Kauffman KJ, Umbaugh CS, Frey SL, Legleiter J. The interaction of polyglutamine peptides with lipid membranes is regulated by flanking sequences associated with huntingtin. *J Biol Chem*. 2013; 288: 14993–15005. <https://doi.org/10.1074/jbc.M112.446237> PMID: 23572526
31. Garten M, Prévost C, Cadart C, Gautier R, Bousset L, Melki R, et al. Methyl-branched lipids promote the membrane adsorption of  $\alpha$ -synuclein by enhancing shallow lipid-packing defects. *Phys Chem Chem Phys*. 2015; 17: 15589–15597. <https://doi.org/10.1039/c5cp00244c> PMID: 25824255
32. Evangelisti E, Cecchi C, Cascella R, Sgromo C, Becatti M, Dobson CM, et al. Membrane lipid composition and its physicochemical properties define cell vulnerability to aberrant protein oligomers. *J Cell Sci*. 2012; 125: 2416–2427. <https://doi.org/10.1242/jcs.098434> PMID: 22344258
33. Bock JE, Gavenonis J, Kritzer JA. Getting in shape: Controlling peptide bioactivity and bioavailability using conformational constraints. *ACS Chemical Biology*. 2013. pp. 488–499. <https://doi.org/10.1021/cb300515u> PMID: 23170954
34. Tsomaia N. Peptide therapeutics: Targeting the undruggable space. *Eur J Med Chem*. 2015; 94: 459–470. <https://doi.org/10.1016/j.ejmech.2015.01.014> PMID: 25591543

35. Usmani SS, Bedi G, Samuel JS, Singh S, Kalra S, Kumar P, et al. THPdb: Database of FDA-approved peptide and protein therapeutics. *PLoS One*. 2017; 12: e0181748. <https://doi.org/10.1371/journal.pone.0181748> PMID: 28759605
36. Pemberton S, Madiona K, Pieri L, Kabani M, Bousset L, Melki R. Hsc70 protein interaction with soluble and fibrillar  $\alpha$ -synuclein. *J Biol Chem*. 2011; 286: 34690–34699. <https://doi.org/10.1074/jbc.M111.261321> PMID: 21832061
37. Redeker V, Pemberton S, Bienvenu W, Bousset L, Melki R. Identification of protein interfaces between  $\alpha$ -synuclein, the principal component of Lewy bodies in Parkinson disease, and the molecular chaperones human Hsc70 and the yeast Ssa1p. *J Biol Chem*. 2012; 287: 32630–32639. <https://doi.org/10.1074/jbc.M112.387530> PMID: 22843682
38. Nury C, Redeker V, Dautrey S, Romieu A, Van Der Rest G, Renard PY, et al. A novel bio-orthogonal cross-linker for improved protein/protein interaction analysis. *Anal Chem*. 2015; 87: 1853–1860. <https://doi.org/10.1021/ac503892c> PMID: 25522193
39. Gao X, Carroni M, Nussbaum-Krammer C, Mogk A, Nillegoda NB, Szlachcic A, et al. Human Hsp70 Disaggregase Reverses Parkinson's-Linked  $\alpha$ -Synuclein Amyloid Fibrils. *Mol Cell*. 2015; 59: 781–793. <https://doi.org/10.1016/j.molcel.2015.07.012> PMID: 26300264
40. Pieri L, Madiona K, Bousset L, Melki R. Fibrillar  $\alpha$ -synuclein and huntingtin exon 1 assemblies are toxic to the cells. *Biophys J*. 2012 Jun 20; 102(12):2894–905. <https://doi.org/10.1016/j.bpj.2012.04.050> PMID: 22735540
41. Pieri L, Madiona K, Melki R. Structural and functional properties of prefibrillar  $\alpha$ -synuclein oligomers. *Sci Rep*. 2016 Apr 14; 6:24526. <https://doi.org/10.1038/srep24526> PMID: 27075649
42. Bendifallah M, Redeker V, Monsellier E, Bousset L, Bellande T, Melki R. Interaction of the chaperones alpha B-crystallin and CHIP with fibrillar alpha-synuclein: Effects on internalization by cells and identification of interacting interfaces. *Biochem Biophys Res Commun*. 2020 Jun 30; 527(3):760–769. <https://doi.org/10.1016/j.bbrc.2020.04.091> PMID: 32430178
43. Wang LH, Rothberg KG, Anderson RG. Mis-assembly of clathrin lattices on endosomes reveals a regulatory switch for coated pit formation. *J Cell Biol*. 1993 Dec; 123(5):1107–17. <https://doi.org/10.1083/jcb.123.5.1107> PMID: 8245121
44. West MA, Bretscher MS, Watts C. Distinct endocytotic pathways in epidermal growth factor-stimulated human carcinoma A431 cells. *J Cell Biol*. 1989 Dec; 109(6 Pt 1):2731–9. <https://doi.org/10.1083/jcb.109.6.2731> PMID: 2556406
45. Freeman D, Cedillos R, Choyke S, Lukic Z, McGuire K, Marvin S, et al. Alpha-synuclein induces lysosomal rupture and cathepsin dependent reactive oxygen species following endocytosis. *PLoS One*. 2013 Apr 25; 8(4):e62143. <https://doi.org/10.1371/journal.pone.0062143> PMID: 23634225
46. Jiang P, Gan M, Yen SH, McLean PJ, Dickson DW. Impaired endo-lysosomal membrane integrity accelerates the seeding progression of  $\alpha$ -synuclein aggregates. *Sci Rep*. 2017 Aug 9; 7(1):7690. <https://doi.org/10.1038/s41598-017-08149-w> PMID: 28794446
47. Flavin WP, Bousset L, Green ZC, Chu Y, Skarpathiotis S, Chaney MJ, et al. Endocytic vesicle rupture is a conserved mechanism of cellular invasion by amyloid proteins. *Acta Neuropathol*. 2017 Oct; 134(4):629–653. <https://doi.org/10.1007/s00401-017-1722-x> PMID: 28527044
48. Zhu X, Zhao X, Burkholder WF, Gragerov A, Ogata CM, Gottesman ME, et al. Structural Analysis of Substrate Binding by the Molecular Chaperone DnaK. *Science* (80-). 1996; 272: 1606–1614. <https://doi.org/10.1126/science.272.5268.1606> PMID: 8658133
49. Roan NR, Sowinski S, Münch J, Kirchhoff F, Greene WC. Aminoquinoline surfen inhibits the action of SEVI (Semen-derived Enhancer of Viral Infection). *J Biol Chem*. 2010; 285: 1861–1869. <https://doi.org/10.1074/jbc.M109.066167> PMID: 19897482
50. Freilich R, Arhar T, Abrams JL, Gestwicki JE. Protein-Protein Interactions in the Molecular Chaperone Network. *Acc Chem Res*. 2018; 51: 940–949. <https://doi.org/10.1021/acs.accounts.8b00036> PMID: 29613769
51. Rosenzweig R, Nillegoda NB, Mayer MP, Bukau B. The Hsp70 chaperone network. *Nat Rev Mol Cell Biol*. 2019; 20: 665–680. <https://doi.org/10.1038/s41580-019-0133-3> PMID: 31253954
52. Arispe N, De Maio A. ATP and ADP modulate a cation channel formed by Hsc70 in acidic phospholipid membranes. *J Biol Chem*. 2000; 275: 30839–30843. <https://doi.org/10.1074/jbc.M005226200> PMID: 10899168
53. Calderwood SK, Theriault J, Gray PJ, Gong J. Cell surface receptors for molecular chaperones. *Methods*. 2007; 43: 199–206. <https://doi.org/10.1016/j.ymeth.2007.06.008> PMID: 17920516
54. Araghi RR, Bird GH, Ryan JA, Jenson JM, Godes M, Pritz JR, et al. Iterative optimization yields Mcl-1–targeting stapled peptides with selective cytotoxicity to Mcl-1–dependent cancer cells. *Proc Natl Acad Sci U S A*. 2018; 115: E886–E895. <https://doi.org/10.1073/pnas.1712952115> PMID: 29339518

55. Bernal F, Tyler AF, Korsmeyer SJ, Walensky LD, Verdine GL. Reactivation of the p53 tumor suppressor pathway by a stapled p53 peptide. *J Am Chem Soc.* 2007; 129: 2456–2457. <https://doi.org/10.1021/ja0693587> PMID: 17284038
56. Jacobsen Ø, Maekawa H, Ge NH, Görbitz CH, Rongved P, Ottersen OP, et al. Stapling of a 310-helix with click chemistry. *J Org Chem.* 2011; 76: 1228–1238. <https://doi.org/10.1021/jo101670a> PMID: 21275402
57. Reverdatto S, Burz D, Shekhtman A. Peptide Aptamers: Development and Applications. *Curr Top Med Chem.* 2015; 15: 1082–1101. <https://doi.org/10.2174/1568026615666150413153143> PMID: 25866267
58. Ghee M, Melki R, Michot N, Mallet J. PA700, the regulatory complex of the 26S proteasome, interferes with  $\alpha$ -synuclein assembly. *FEBS J.* 2005; 272: 4023–4033. <https://doi.org/10.1111/j.1742-4658.2005.04776.x> PMID: 16098186
59. Whitmore L, Wallace BA. DICHROWEB, an online server for protein secondary structure analyses from circular dichroism spectroscopic data. *Nucleic Acids Res.* 2004; 32: W668–W673. <https://doi.org/10.1093/nar/gkh371> PMID: 15215473
60. Wanker EE, Scherzinger E, Volker H, Sittler A, Eickhoff H, Lehrach H. Membrane Filter Assay for Detection of Amyloid-like Polyglutamine-Containing Protein Aggregates. *Methods Enzymol.* 1999; 309: 375–386. [https://doi.org/10.1016/s0076-6879\(99\)09026-6](https://doi.org/10.1016/s0076-6879(99)09026-6) PMID: 10507036
61. Schindelin J, Arganda-Carreras I, Frise E, Kaynig V, Longair M, Pietzsch T, et al. Fiji: An open-source platform for biological-image analysis. *Nature Methods.* 2012. pp. 676–682. <https://doi.org/10.1038/nmeth.2019> PMID: 22743772
62. Rueden CT, Schindelin J, Hiner MC, DeZonia BE, Walter AE, Arena ET, et al. ImageJ2: ImageJ for the next generation of scientific image data. *BMC Bioinformatics.* 2017; 18: 529. <https://doi.org/10.1186/s12859-017-1934-z> PMID: 29187165